AFRL-RV-PS-
TR-2018-0117

RADIO FREQUENCY LOCALIZATION OF A TRANSMITTER USING MULTIPLE SPACE-BASED RECEIVERS

Gregory Durgin

Georgia Tech Research Corporation
505 10th Street NW
Atlanta, GA 30318-5775

08 October 2018

Final Report

APPROVED FOR PUBLIC RELEASE; DISTRIBUTION IS UNLIMITED.

AIR FORCE RESEARCH LABORATORY
Space Vehicles Directorate
3550 Aberdeen Ave SE
AIR FORCE MATERIEL COMMAND
KIRTLAND AIR FORCE BASE, NM 87117-5776

DTIC COPY
NOTICE AND SIGNATURE PAGE

Using Government drawings, specifications, or other data included in this document for any purpose other than Government procurement does not in any way obligate the U.S. Government. The fact that the Government formulated or supplied the drawings, specifications, or other data does not license the holder or any other person or corporation; or convey any rights or permission to manufacture, use, or sell any patented invention that may relate to them.

This report is the result of contracted fundamental research which is exempt from public affairs security and policy review in accordance with AFI 61-201, paragraph 2.3.5.1. This report is available to the general public, including foreign nationals. Copies may be obtained from the Defense Technical Information Center (DTIC) (http://www.dtic.mil).

AFRL-RV-PS-TR-2018-0117 HAS BEEN REVIEWED AND IS APPROVED FOR PUBLICATION IN ACCORDANCE WITH ASSIGNED DISTRIBUTION STATEMENT.

//signed//

THOMAS LOVELL
Program Manager

//signed//

DAVID WILT
Tech Advisor, Spacecraft Components Technology Branch

//signed//

JOHN BEAUCHEMIN
Chief Engineer, Spacecraft Technology Division
Space Vehicles Directorate

This report is published in the interest of scientific and technical information exchange, and its publication does not constitute the Government's approval or disapproval of its ideas or findings.

Approved for public release; distribution is unlimited.

REPORT DOCUMENTATION PAGE

Form Approved
OMB No. 0704-0188

1. REPORT DATE *(DD-MM-YYYY)*	**2. REPORT TYPE**	**3. DATES COVERED** *(From - To)*
08/10/2018	Final Report	07 Jul 2015 – 08 Oct 2018

4. TITLE AND SUBTITLE
Radio Frequency Localization of a Transmitter using Multiple Space-Based Receivers

5a. CONTRACT NUMBER
FA9453-15-1-0311

5b. GRANT NUMBER

5c. PROGRAM ELEMENT NUMBER
62601F

6. AUTHOR(S)
Gregory Durgin

5d. PROJECT NUMBER
8809

5e. TASK NUMBER
PPM00020772

5f. WORK UNIT NUMBER
EF125834

7. PERFORMING ORGANIZATION NAME(S) AND ADDRESS(ES) AND ADDRESS(ES)
Georgia Tech Research Corporation
505 10th Street NW
Atlanta, GA 30318-5775

8. PERFORMING ORGANIZATION REPORT NUMBER

9. SPONSORING / MONITORING AGENCY NAME(S) AND ADDRESS(ES)
Air Force Research Laboratory
Space Vehicles Directorate
3550 Aberdeen Ave., SE
Kirtland AFB, NM 87117-5776

10. SPONSOR/MONITOR'S ACRONYM(S)
AFRL/RVSV

11. SPONSOR/MONITOR'S REPORT NUMBER(S)
AFRL-RV-PS-TR-2018-0117

12. DISTRIBUTION / AVAILABILITY STATEMENT
Approved for public release; distribution is unlimited.

13. SUPPLEMENTARY NOTES

14. ABSTRACT
The end result of this research is expected to show which applications space-based geo-location is suitable for, as well as overall feasibility. This will be a novelty, as there has been relatively little research made in this area by the scientific community overall. The technical approach will consist primarily of theoretical work and simulation, with a possibility of some minimal laboratory work later on. The research will involve work in signal processing, applied electromagnetics, orbital mechanics, and statistical estimation.

15. SUBJECT TERMS
Signal Processing; Antenna Design; Uncooperative RF Geolocation; Direction Of Arrival; DOA; Frequency Ratio Of Arrival

16. SECURITY CLASSIFICATION OF:			**17. LIMITATION OF ABSTRACT**	**18. NUMBER OF PAGES**	**19a. NAME OF RESPONSIBLE PERSON**
					Thomas Lovell
a. REPORT	**b. ABSTRACT**	**c. THIS PAGE**			**19b. TELEPHONE NUMBER** *(include area code)*
Unclassified	Unclassified	Unclassified	Unlimited	36	

(This page intentionally left blank)

TABLE OF CONTENTS

Section **Page**

LIST OF FIGURES

Figure **Page**

ACKNOWLEDGMENT

This work was supported in part by the Air Force Research Laboratory (AFRL) under Grant FA9453-15-1-0311. The U.S. Government is authorized to reproduce and distribute reprints for Governmental purposes notwithstanding any copyright notation thereon.

DISCLAIMER

The views and conclusions contained herein are those of the authors and should not be interpreted as necessarily representing the official policies or endorsements, either expressed or implied, of AFRL or the U.S. Government.

1.0 SUMMARY

The objective of this research was to determine how a small cluster of cubesat-based receivers can use passive radio frequency (RF) localization techniques to locate an uncooperative transmitter on the earth or in orbit. This process consisted of first determining an initial region of interest (ROI) in which the transmitter is located; next channel modeling, which will account for various sources of signal error; then parameter estimation, where time difference of arrival (TDOA) and frequency difference of arrival (FDOA) values and their respective covariances are obtained; finally, the RF localization equations are solved for a position or orbit, but if not enough information is available for a complete solution, a constrained admissible region (CAR) of possible orbits is obtained. The research includes a thorough error analysis, and an investigation of the use of employing constrained admissible regions (CAR) to solve the space-to-space localization problem.

2.0 INTRODUCTION

The objective of this research was to determine how a small cluster of cubesat-based receivers can use uncooperative radio frequency (RF) localization techniques to locate an uncooperative transmitter on earth or in space. This process consisted of first determining an initial region of interest in which the transmitter was located; next channel modeling, which will account for various sources of signal error; then parameter estimation, where time difference of arrival (TDOA) and frequency difference of arrival (FDOA) values and covariances were obtained; finally, the RF localization equations were solved for a position or orbit, but if not enough information is available for a complete solution, a constrained admissible region (CAR) is obtained.

2.1 Origin and History of the Problem

RF localization techniques have been used at least since the early 1900s for ranging of metallic objects [1], even prior to the advent of radar in the 1930s [2]. In 1957 Russia launched the world's first artificial satellite Sputnik 1. Researchers in the United States were able to determine the orbit of Sputnik because of the 20.005 MHz and 40.002 MHz tones that it was transmitting [3]. A decade later, in 1967, the US Navy launched the Transit Satellite Constellation, known as NAVSAT. NAVSAT used the same concept of Doppler shift from multiple satellites to serve as an early global positioning system for ships. The first search and rescue satellite-aided tracking (SARSAT) satellite was launched in 1982, and the system is still in use today. SARSAT also exploited the Doppler Effect; however, the SARSAT satellites were now acting as receivers, listening for distress beacons on the ground [4]. The first satellite in the Global Positioning System (GPS) constellation was launched in 1978. The GPS satellites broadcast timed signals that are known to the receivers, which in turn use this time of arrival information [5]. GPS has become the dominant navigation and positioning system for both military and civilian use worldwide.

There are many reasons why RF localization is desirable from a space-based platform. The time difference of arrival (TDOA) method of RF localization has been used by the FCC on the ground to locate jammers, and NOAA has employed frequency difference of arrival (FDOA) with the

SARSAT constellation for search and rescue for decades. There are, however, cases where the area that needs to be searched is too large, remote, or dangerous to do the localization on the ground. More recently applications of uncooperative RF localization requiring a space-based platform have been proposed [6]. The space-based platform introduces many unique challenges such as size, weight, and power constraints; signal strength, sensitivity, and interference issues; Doppler shifts and other effects caused by receiver motion; and the effects of space weather [7][8].

Cooperative RF localization refers to localization schemes where there is some type of cooperation between the transmitter and the receiver. The global navigation satellite systems (GNSS), including the US's GPS, Russia's GLONASS, and Europe's Galileo constellations, are examples of cooperative RF localization, where there is coordination between the transmitters and the receivers. Timed signals are broadcast from the satellite-based transmitters in orbit, whereby a receiver can locate itself on the surface of a sphere using the time of arrival information [5].

Uncooperative RF localization requires minimal or no coordination between the transmitter and the receivers, so it is useful in finding jammers and more benign interfering sources, navigation, search and rescue, as well as other applications. The SARSAT system and the now-discontinued Loran-C, are examples of uncooperative RF localization [4], both systems utilized simple and untimed signals.

2.2 Uncooperative Radio Frequency Localization

2.2.1 Techniques of Uncooperative Radio Frequency Localization.

Not all methods of uncooperative RF localization have the same precision. Typically, methods can be broken down into two categories: coarse methods, and precision methods. Coarse RF localization methods are usually used to obtain a direction of arrival. This direction of arrival can be obtained many different ways, though the most precise is the interferometery method, which requires a phased array. There are other methods, such as relative signal strength. The two precision methods of uncooperative RF localization: the TDOA method and the FDOA method.

2.2.1.1 Time Difference of Arrival.

The TDOA method of localization is described in detail in other literature, such as [2][9]. Here, only a brief summary of the method will be given. TDOA measurements are obtained by cross correlating the signal received by two displaced receivers; the TDOA is the lag value at which the cross correlation is at its maximum. (1) is the TDOA equation, where c is the speed of light; Δt_{ij} is the TDOA between receivers i and j; x_i, y_i, and z_i are the Cartesian coordinates of the receiver i; x_j, y_j, and z_j are the Cartesian coordinates of the receiver j; and x, y, and z are the Cartesian coordinates of the transmitter.

$$c\Delta t_{ij} = \sqrt{(x_i - x)^2 + (y_i - y)^2 + (z_i - z)^2} - \sqrt{(x_j - x)^2 + (y_j - y)^2 + (z_j - z)^2} \quad (1)$$

(1) has the form of a hyperbola in two-dimensions and a two-sheeted hyperboloid in three-dimensions, with the two receivers at the foci and the transmitter located somewhere on the surface. The geometric position of a transmitter can be found by intersecting multiple TDOA hyperboloids [9]. Note that multiplying TDOA by the speed of light yields the range difference. The now-discontinued Loran-C is an example of a system that employed the TDOA method for maritime navigation.

2.2.1.2 Frequency Difference of Arrival.

Like with TDOA, the FDOA method requires two receivers and a transmitter. FDOA can be used when either the transmitter or at least one of the two receivers is in motion. There are different formulations of FDOA, and the equations become more complex as the number of objects in motion increases. For this reason, FDOA is usually used for scenarios where the receivers are stationary and the transmitter is in motion, when the transmitter is stationary and one of the receivers is in motion, or when the transmitter is stationary and both of the transmitters are in motion [2], though, formulations do exist for when the transmitter is stationary and both receivers are in motion. The geometric surface on which the transmitter lies looks similar to electric field lines in three-dimensions, with the receivers being the positive and negative charges. All formulations of the FDOA problem can be derived from the Doppler equation, (2), where f_i is the received frequency at receiver i, f_0 is the transmitted frequency, v_i is the velocity of receiver i, r_i is the position of receiver i, and c is the speed of light. The SARSAT system, which is currently used for search and rescue, is an example of an application that uses the FDOA method.

$$f_i = f_0\left(1 + \frac{\vec{v}_i \cdot \vec{r}_i}{c\|\vec{r}_i\|}\right) \quad (2)$$

2.2.1.3 Direction of Arrival.

While direction of arrival—also commonly referred to in literature as angle of arrival—is not technically a precision method of radio frequency localization, it can be used in conjunction with the TDOA and FDOA methods to refine the solution. For most cases of disambiguation, the tight 1 degree uncertainty of a phased array is not needed. (3) is the two-dimensional angle of

arrival equation, where θij is the angle of arrival between antenna elements i and j, dij is the distance between elements i and j, δtij is the time difference of arrival between elements i and j, and c is the speed of light. The direction of arrival is typically found using the multiple signal classification (MUSIC) algorithm with multiple angles of arrival from a phased array. The Full Sky Array project—being done by the Air Force Research Laboratory (AFRL) and the University of New Mexico—to catalog all satellites within line of sight of the array on the earth is an example of a project that currently uses the Direction of Arrival (DOA) method.

$$\theta_{ij} = \cos^{-1}\left(\frac{c\delta t_{ij}}{d_{ij}}\right) \tag{3}$$

2.2.2 Space-Based Radio Frequency Localization Scenarios.

There are two basic RF localization scenarios that the research in this proposal intends to address: ground-to-space localization scenarios and space-to-space localization scenarios.

2.2.2.1 Ground-to-Space Localization.

Ground-to-space RF localization—also known as geolocation—includes all scenarios where a space-based platform is used to locate a ground-based transmitter. In these scenarios, the transmitter could be stationary, in motion, or undergoing acceleration. There could also be more than one transmitter. However, for the research planned and undertaken in this proposal, there is assumed to be a single, stationary transmitter. Applications of ground-to-space localization include any scenario where the region of interest is too large, too remote, or too dangerous to be surveyed by ground or air vehicles.

2.2.2.2 Space-to-Space Localization.

Space-to-space RF localization is the use of space-based receivers to locate a space-based transmitter, which in most cases will be in a closed orbit around the earth. Unlike geolocation, space-to-space localization becomes an orbit determination problem requiring both position and velocity information, thus there are many different combinations of measurements and ways of formulating this problem, and only a few have been explored. The field of space-to-space localization is still in its infancy; the capabilities, limitations, and applications will likely become more clear as this area of research progresses.

While there have been several real-world examples of the TDOA and the FDOA methods used separately for RF localization applications, applications employing a combination of the TDOA and FDOA methods have the potential for a greater degree of accuracy than either method has by itself. Such a combination of localization techniques is particularly desirable for space-to-space localization. Interest in space-to-space RF localization has substantially increased in recent

years, on the part of the US military and others [7][9]. This increase in interest likely has multiple causes. For decades the USA and Russia had a monopoly on space, but this has changed dramatically now that China and Europe have substantial space programs in their own right, and this trend will continue as more countries develop space programs of their own, and as companies like SpaceX and Virgin Galactic increase their presence in space. Space is becoming more crowded, and space-to-space localization could be used for navigating this environment as well as for space situational awareness applications.

There is also the problem of space debris, which is increasing exponentially, with two major increases when a US satellite crashed into a decommissioned Russian satellite and when China destroyed one of their satellites in orbit [10]. Space is more crowded now than it ever has been, and this trend is only going to increase. Space-to-space RF localization could potentially be used to catalog and track both satellites and space debris. It has many military and civilian applications for navigating the crowded space environment, space situational awareness, and tracking down space-borne jammers.

2.2.3 Solutions to the Localization Equations.

The TDOA and FDOA equations represent surfaces in three-dimensional space, on which the transmitter is located. These surfaces are described by non-polynomial equations, which make them difficult to solve. There are various numerical and iterative techniques that can be employed, each with their own set of limitations. In practice, the cross ambiguity function is employed in most real-world RF localization applications, this process is, however, computationally expensive. Deriving novel methods of solving these equations is not a focus of this research. The methods of solving these equations employed in this research included Newton-Raphson iteration, the Macaulay Resultant [8], and the software package Bertini..

3.0 METHODS, ASSUMPTIONS, AND PROCEDURES

3.1 Radio Frequency Localization

The methods of DOA, TDOA, and FDOA have been used for many different applications, and have likewise been further developed; a thorough overview of these developments is beyond the scope of this work, however, some areas directly related to this proposal will now be considered. Because the TDOA and FDOA equations are non-polynomial in nature, efforts have been made to find a fast and accurate way to solve these equations for a point solution [8]. There are various formulations for the TDOA problem [9]: TDOA was originally implemented using fixed receiver stations [1], there have also been formulations for having one fixed receiver and one moving one [6], recently formulations are becoming more common for the transmitter and both receivers to be moving [7]. For DOA measurements, the multiple-signal identification and classification algorithm has become the standard for processing phased array data [11]. The cross-ambiguity function is commonly employed to solve systems that utilize a fusion of TDOA and FDOA measurements; it is essentially a two dimensional cross correlation that minimizes error in both measurements [9]. Dilution of precision is another topic that is commonly found in the literature for nearly all RF localization techniques [2].

3.2 Space-Based Radio Frequency Localization

The DOA and TDOA methods of RF localization date back to the military advances in RF technology during World War II [2]. The FDOA method has always primarily been associated with RF localization relating to space, and dates back to Sputnik 1 [3]. Since these techniques of uncooperative RF localization have existed for roughly 80 years, much literature has been published over the years; thus, this literature survey will focus on more recent publications relating to uncooperative space-based RF localization. The first proposed use of TDOA for space-based applications was by Escobal et. al. in 1975 [12], where five stationary ground-based receivers, taking simultaneous measurements, are used to localize a single space-based transmitter. Ho and Chan in 1993 proposed a TDOA geolocation system, requiring three or four geostationary satellites (four if the transmitter's altitude is unknown) to locate a ground-based transmitter. This method uses a surface-of-the-earth constraint to eliminate ambiguity, and they use a non-iterative method to solve the equations [6]. In 1994 Ho and Chan improved their system somewhat, but it still requires that the three TDOA hyperboloids have a common focus, which means four satellites taking simultaneous measurements, one geostationary satellite and one moving satellite taking three separate measurements, or a some other configuration that results in three TDOA hyperboloids with a common focus [13]. Ho and Chan, in 1997, introduced a scheme incorporating both TDOA and FDOA measurements, though still requiring a common focus [14]. Musicki and Koch in 2008 proposed a space-based geolocation scheme [15] based on their prior work on geolocation using unmanned aerial vehicles [16][17]. This scheme uses a combination of TDOA and FDOA measurements found using CAF; CAF greatly increases computational cost because it is in essence, a two-dimensional cross correlation. In 2014, Sinclair et. al. presented a TDOA geolocation method where the Macaulay resultant is used to solve the TDOA equations [8]; this method eliminated the need for a common focus, but the Macaulay method has issues with numerical stability. In 2017, Shuster et. al. published a TDOA space-to-space RF localization method using a minimum of six TDOA measurements collected at two or more moments in time [7]. Most of these papers consider only the method of RF localization for different scenarios, with little or no consideration given to obtaining these TDOA and FDOA measurement or to practicalities of the RF localization system as a whole.

3.3 Error Sources for Space-Based Radio Frequency Systems

Error analysis for space-based RF systems is a huge field of research in and of itself. There are many error sources that apply to all RF systems, and there are error sources that apply to all space-based RF systems. There are error sources that apply to space-to-space links, and there are error sources that apply to space-to-ground links. The goal of error analysis in the proposed research here is not to develop new empirical or analytical error models, rather, to incorporate existing error models into a system of uncooperative RF localization from a space-based platform. Most of the literature that deals with uncooperative methods of RF localization from a space-based platform either mostly ignores error, or error sources are the sole topic [18]. Some good general sources for error sources for space-based RF systems are [19][20][21].

There has also been some literature on how different error sources will affect different RF systems. Hahn derived an expression for TDOA covariance in [22] and expands on it in [23], for example.

3.4 Admissible Regions

In realm of orbit determination using optical measurements of space objects, Gauss's method or Lambert's method can be employed for initial orbit determination with a minimum of three separate measurements. And if the exposure times are sufficiently long that angular rate information is obtained from the 'streaks', only two separate measurements are needed; in other cases, radar information can be combined with optical information, so only one optical image is required for orbit determination. However, there are cases where not enough information is available to satisfy the six-dimensional orbit determination problem. Admissible regions were first introduced by Milani et. al. in 2004 [24].

In cases where not enough information is available to perform conventional orbit determination, an admissible region of all orbits that are possible, given what information is available, can be found. For example, a single optical measurement of a space object yields the angular position—relative to the position of the observer—and angular rate change of the object at a particular epoch in time; however, the orbit, which can be described by the range and range-rate, is still undetermined. But by making assumptions, such as that the object is earth orbiting, an admissible region can be formed—which is typically expressed graphically on the range, range-rate plane. Additional constraints can also be placed on the admissible region, such as energy or inclination, further limiting its size. A sampling of possible orbits in a particular admissible region at a particular epoch can be propagated forward to be compared with the admissible region from another set of measurements at a later epoch to further shrink the region [25].

The admissible region can be represented by a uniform probability density function in an undetermined state space, assuming that the constraining hypotheses are true [26]. Besides the method originally used by Milani, there are several methods available to uniformly sample the admissible region [27][28], but there are also some methods that utilize optimization techniques so that it is not necessary to sample the entire region [29]. Multiple hypotheses filters, or particle filters, can be initialized from a discretized admissible region, and new measurement information can be incorporated into the filter [30]. There have also been developments on probabilistic formulations of constrained admissible regions [31][32]. Gaussian mixture models can be used to approximate an admissible, whereby eliminating the discontinuity at the constraints [32]. Uncertainty arising from error in the measurements and the observer's position can be mapped into state uncertainties for point solutions [33]. From a review of existing literature, it appears that the most common application of admissible regions is to disambiguate different objects in space, that are observed at different times, and often to obtain some kind of rough approximation of what their orbits could be.

While the original literature considered tracking and cataloging asteroids, the space situational awareness community has applied the concept to earth orbiting objects. Tommei et al. applied admissible regions to tracking space debris in earth orbit [34], Maruskin et al. used admissible regions to correlate observations of objects in earth orbit [27]. Fujimoto et al. expanded the technique to include solutions for circular and zero-inclination orbits [28]. DeMars et al. combined the concepts of admissible regions and multiple hypothesis filtering [30]. Fujimoto et al. also addressed to problem of admissible regions, where no useful angular rate information is obtained from the optical measurements [35]. Nearly all of the existing literature on admissible regions has been for admissible regions constructed from optical measurements, though, there has been some work done by Farnocchia et al. on incorporating radar measurements into admissible regions [36], and there has been one publication on using admissible regions for TDOA measurements [37], by Worthy et al.

3.5 Initial Region of Interest

Uncooperative RF localization systems typically do not provide continuous global coverage, so it is necessary to have a pre-defined initial region of interest (ROI), in which the transmitter is located. Thus, techniques for finding an initial ROI for several different scenarios based on minimal data were derived. This ROI, once obtained, can be used for mission design to determine the deployment and maneuvering needed to obtain a precise positioning of transmitter. To this end, four RF localization scenarios are defined here. For all of these scenarios, it is assumed that there is only one transmitter. It should also be noted that these scenarios are not mutually exclusive. For example, a communication link between a satellite in space and a transmitter on the ground could also be intercepted by a receiver also located on the ground, making this both a ground-to-space and a ground-to-ground scenario—assuming that both sources of information are available.

3.5.1 Ground-to-Ground Transmission.

In this scenario, the transmitter located on the ground is transmitting to receivers, which are also located on the ground. For the ground-to-ground scenario, the ROI is found by assuming maximum range of the ground-based transmitter. This, of course, varies by power level, topography, and other conditions. The transmitter could also be on a tower, significantly far off the ground, and for HF frequencies, over the horizon transmission is possible. For many scenarios, line-of-sight transmission can be assumed. It is also assumed that the positions of the ground-based receivers that have access to the transmitted signal are known. Around each ground-based receiver, a circle can be drawn, the radius of which is equal to the assumed maximum range of the transmitter. The initial ROI is the intersection of these circles for each ground-based user.

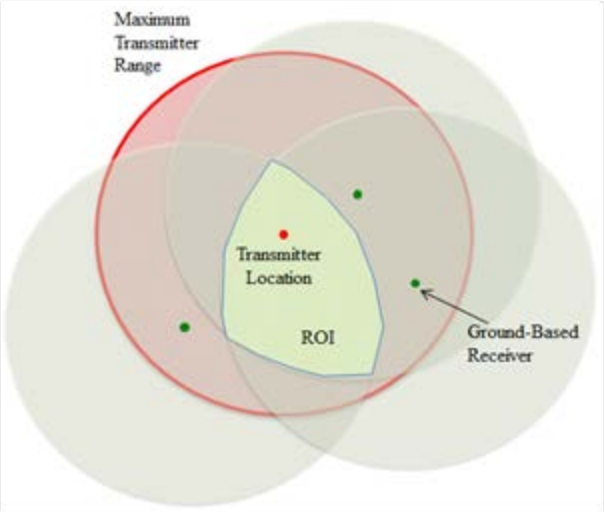

Figure 1. Region of Interest for the Ground-to-Ground Scenario

3.5.2 Ground-to-Space Transmission.

This scenario consists of a transmitter located on the ground, and a receiver located in space. For the ground-to-space transmission scenario, it is assumed that both the ephemeris of the satellite-based receiver, and times that the receiver has access to the ground-based transmitter are known. The area of the earth that the satellite has line-of-sight of is traced-out onto the ground at the beginning of the time interval where the satellite-based receiver has access to the signal. The line-of-sight area at the end of the access time interval is also traced out on the earth. The ROI is the intersection of these two regions. This process can be repeated, further shrinking the ROI, for multiple passes. This process is illustrated in Figure 2.

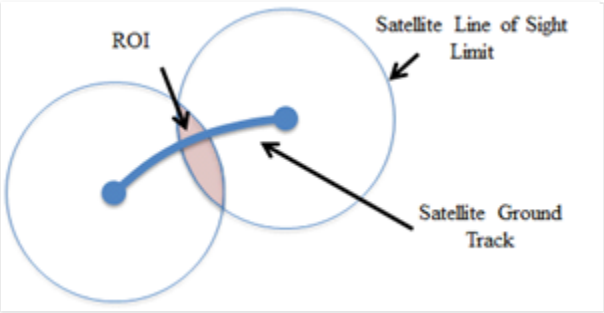

Figure 2. Region of Interest for the Ground-to-Space Scenario

3.5.3 Space-to-Ground Transmission.

The space-to-ground scenario consists of a satellite-based transmitter, and one or more ground based receivers. This could be nearly any conceivable type of link. For the space-to-ground scenario, the ROI is somewhat more complex; the prior two examples involved finding a two-dimensional geometric area. For space-based transmitters, the ROI is partially a three-dimensional volume in space, but this also becomes a kind of orbit determination problem, as the range of possible orbits of the satellite become the actual ROI. It is assumed that the latitude and longitude of the ground-based receiver are known. The ROI is defined by the admissible region constructed by a set of six constraints. This type of ROI does not easily lend itself to a graphical representation. The ROI can be further limited by intersecting the admissible regions found from multiple passes, or by introducing other constraints.

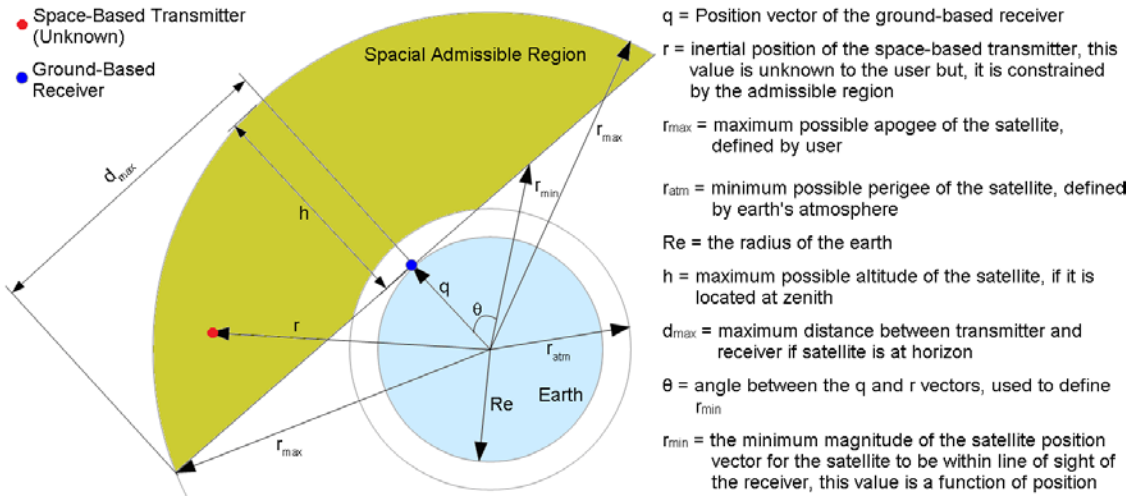

Figure 3. Region of Interest for the Space-to-Ground Scenario

Let $\boldsymbol{q}$ be the position vector of the ground-based receiver; $\boldsymbol{r}$ the inertial position of the satellite-based transmitter; r_{max} is the maximum possible apogee of the satellite; r_{atm} is the minimum possible perigee of the satellite; Re is the radius of the earth; θ is the angle between $\boldsymbol{q}$ and $\boldsymbol{r}$; ρ_{max} is the maximum satellite range; $\boldsymbol{e_E}$, $\boldsymbol{e_N}$, and $\boldsymbol{e_Z}$ are the East, North, and zenith unit vectors describing the topocentric coordinate system at the receiver's position; s_E, s_N, and s_Z are the East, North, and zenith components of the satellite position vector in the topocentric frame; and ε is the specific orbit energy of the satellite. These values are expressed in equations (4)-(8), and this scenario is illustrated in Fig. 3.

$$s_Z \geq 0 \tag{4}$$

$$r_{atm} \leq \|\vec{r}\| \leq r_{\max} \tag{5}$$

$$0 \le \theta \le \cos^{-1}\left(\frac{\mathrm{Re}}{r_{\max}}\right) \tag{6}$$

$$\check{r} \cdot \check{q} \ge \check{q} \cdot \check{q} \tag{7}$$

$$\varepsilon \le \mathbf{O} \tag{8}$$

3.5.4 Space-to-Space Transmission.

A space-to-space scenario can be any conceivable where there is a single satellite based transmitter and one or more satellite-based receivers. The ROI for the space-to-space scenario is similar to the ROI for the space-to-ground scenario, in that it is found using a modified version of the method of constrained admissible regions. Like the ROI for the space-to-ground transmission scenario, the ROI for the space-to-space scenario is also defined by a set of constraints, (9)-(12), where *h* is the altitude of the space-based receiver, and all other variables are the same as was defined in the previous subsection.

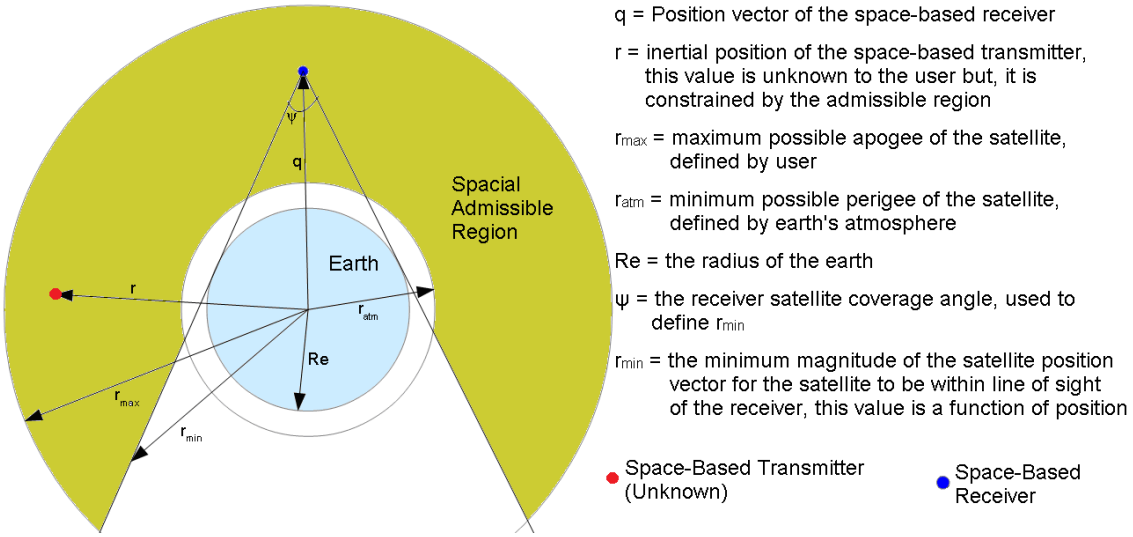

Figure 4. Region of Interest for the Space-to-Space Scenario

$$s_Z \ge \mathrm{Re}\cos\left(90° - \sin^{-1}\left(\frac{\mathrm{Re}}{\mathrm{Re}+h}\right)\right) \tag{9}$$

$$\sqrt{s_N^2 + s_E^2} \ge \frac{\cos\left(90° - \sin^{-1}\left(\frac{\mathrm{Re}}{\mathrm{Re}+h}\right)\right)}{\sin\left(90° - \sin^{-1}\left(\frac{\mathrm{Re}}{\mathrm{Re}+h}\right)\right)} s_Z \tag{10}$$

$$r_{atm} \le \left\|\check{r}\right\| \le r_{\max} \tag{11}$$

$$\varepsilon \le \mathbf{O} \tag{12}$$

3.6 Minimum Time Difference of Arrival Accumulation Time

Another important concept for TDOA RF localization is that of minimum signal accumulation time. An expression for TDOA covariance, (2), was derived by Hahn in [22] using the Cramer-Rao lower bound (CRLB), and since has widely been used for TDOA applications [23][13].

$$\sigma_{TDOA}^2 \geq \frac{2\pi}{T_{accum}} \left\{ \int_B d\omega \omega^2 \left[\frac{(S_1/N_1)(S_2/N_2)}{1+(S_1/N_1)+(S_2/N_2)} \right] \right\}^{-1} \tag{13}$$

Where σ_{TDOA} is the TDOA measurement error standard deviation, T_{accum} is the signal accumulation time, B is the signal bandwidth, ω is the angular frequency variable, S_1 and S_2 are the signal power spectral densities at receivers 1 and 2 respectively, and N_1 and N_2 are the noise power spectral densities at receivers 1 and 2 respectively. The lower limit of the equality is the CRLB. A perfectly efficient estimator would achieve this bound in its estimate of the TDOA value, assuming all error is captured by the signal-to-noise ratios. (13) can be used to obtain the detection equation, (14), which gives the minimum signal accumulation time for a given carrier-to-noise ratio and sampling period.

$$T_{accum} \geq 16 \left[\frac{1 + \Delta t_{samp} \left[(C/N_0)_1 + (C/N_0)_2 \right]}{\Delta t_{samp} (C/N_0)_1 (C/N_0)_2} \right] \tag{14}$$

Where Δt_{samp} is the sampling period, and $(C/N_0)_1$ and $(C/N_0)_2$ are the carrier-to-noise-density ratios—in hertz–of receivers 1 and 2 respectively. Making the sampling period small causes the minimum accumulation time to become large. Because this inequity describes the minimum accumulation time for a cross correlation, the carrier-to-noise ratios for both receivers effect the value, both receivers must use the same accumulation time.

3.7 Error Analysis

3.7.1 Sources of Error.

The error sources that affect measurement error, and in turn solution error, can be broken down into three categories: environmental error sources, receiver and positioning error sources, and error introduced by the movement of the satellite-based receivers.

3.7.1.1 Error Introduced by the Earth and Space Environment.

The sources of error considered include refraction, attenuation, humidity, reflection, multipath, diffraction, fading, scattering, dispersion, ionospheric effects, tropospheric effects, and relativistic effects. Atmospheric attenuation, consists primarily of oxygen absorption and water absorption; existing empirical models were tested for both of these. Attenuation as a function of altitude was also considered and applied; attenuation is not linear with altitude, but it is approximately linear with atmospheric density. The differences between liquid water and ice attenuation were also considered. The attenuation for the dry gasses in the atmosphere, as well as for moisture in the atmosphere are expressed in equations (15) and (16) respectively, where α_{db} is the specific attenuation, and α in equation (17) is the specific extinction coefficient, either can be obtained from a table or figure of data for given conditions and frequencies.

$$L_{gas,db} = \int_{path} \alpha_{gas,db} dl \tag{15}$$

$$L_{rain,db} = \int_{path} \alpha_{rain,db} dl \tag{16}$$

$$\alpha_{db} = 4.34\alpha \tag{17}$$

Some preliminary work was also done on the effects of multipath interference, consisting of reflections off the surface of the earth. A way to incorporate multipath would be to export a far field mapping from CST, and use this mapping for the beam pattern in the end to end simulation. The effects of scattering from ionospheric plasma bubbles and GPS scintillations were also considered, though, at the present these effects are being ignored, as they only seem to present a problem for GPS during times of high solar activity. Troposphere delay is another environmental effect considered; it is non-frequency dependent, so tropospheric delay can only be accounted for by using atmospheric models and observational data. (18) and (19) are the hydrostatic and wet components of tropospheric delay respectively; where H is the height above sea-level, k_1 is 77.604 K/mbar, R_d is 287.0564 J/kg/K, g_m is 9.784 m/s^2, g is 9.80665 m/s^2, and k_2 is 382,000 K^2/mbar. (20) $T_{troposphere}$ is the mean tropospheric delay.

$$T_{Z,dry} = \left[1 - \frac{\beta H}{T}\right]^{\frac{g}{R_d \beta}} \frac{10^{-6} k_1 R_d P}{g_m} \tag{18}$$

$$T_{Z,wet} = \left[1 - \frac{\beta H}{T}\right]^{\frac{(\lambda+1)g}{R_d \beta} - 1} \frac{10^{-6} k_2 R_d P}{(\lambda+1) g_m - \beta R_d} \frac{e}{T} \tag{19}$$

$$T_{Troposphere} = \left(T_{Z,dry} + T_{Z,wet}\right) \frac{1.001}{\sqrt{0.002001 + \sin^2(E)}} \tag{20}$$

The Klobuchar Ionospheric Model was used for modeling ionospheric delay [38].

3.7.1.2 Receiver Synchronization and Positioning Error.

Receiver error could be used to refer to the noise figure associated with the satellite-based receivers. Treating this error as white Gaussian noise is a coarse way of describing this error. A more precise way would be to break the receiver into clock drift, jitter, and amplitude noise at the signal level. Receiver error is a part of measurement error, but it is largely dependent on the specific receiver that is used. Positioning error is related to the level of precision that can be known of the satellite-based receivers' absolute position. This could be limited to the level of precision available using GPS, or more advanced techniques could be employed to increase the precision.

3.7.1.3 Error Introduced by Satellite Motion.

In cases where the receivers are located on satellites in low earth orbit (LEO), speeds are great enough that the distances that the receivers travel during the time it takes to make TDOA measurements is significant. The user can assume that the measurement data corresponds to the center of the distance traveled by the receivers, but this assumption will introduce error to the overall problem.

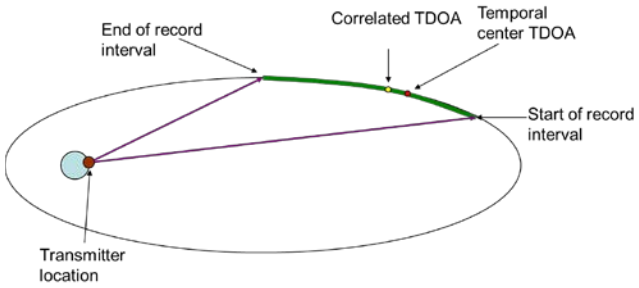

Figure 5. Localization Scenario Involving Two Space-Based Receivers. Receiver Satellites are on the Same Orbital Path. Direction of Orbital Motion is Counter-Clockwise

The TDOA error induced by satellite-based receiver motion arises from the fact that both receivers are moving. This means that the range between the transmitter and the receivers is constantly changing, which means that the receiver positions and the true TDOA will be different at the beginning and at the end of the record interval, and at every point in between. There will be a Doppler shift—which will also be changing, due to the perpetual acceleration experienced by all orbiting bodies—that will result in a flattening and widening of the peak in the cross correlation, thus increasing error in the TDOA measurement. Both this change in receiver positions and Doppler effects contribute to TDOA error, and thus overall solution error; these issues arise from the fact that satellite-based receivers are being considered. This problem was explored in [18].

3.7.2 Measurement Error.

Here measurement error refers to the sigma error associated with the direct TDOA and FDOA measurements. The error sources in the previous subsection primarily affect measurement error. Measurement error can further be broken down into three nonexclusive types: signal attenuation, which lowers SNR; noise, that also lowers SNR; and delays, which directly add to the TDOA measurements. Signal attenuation is captured in the link budget equation, (21), where *L* is the attenuation term.

$$P_r = \frac{P_t G_t(\theta_t, \phi_t) G_r(\theta_r, \phi_r) \lambda^2}{4\pi r^2} L \tag{21}$$

The noise sources can generally be treated as additive white Gaussian noise centered at zero, because most of the time the non-zero bias will either be known, or can be canceled out using a model. The same is true for the delay error; the non-zero bias can be canceled out using analytical or empirical models.

3.7.3 Solution Error.

Solution error is the sigma value associated with the RF localization solution; this would be affected by the measurement error, as well as the dilution of precision that is related to the receivers' positions relative to the transmitter. Over the course of a pass, the RF localization satellites will likely generate a large number of point solutions that could potentially be refined into a more accurate overall solution using some form of least squares estimation or Kalman filtering, though little work has been done in this area.

3.8 Ground-to-Space Radio Frequency Localization

One objective that has been accomplished is that an end-to-end simulator was coded in Matlab to solve the ground-to-space localization problem using TDOA measurements. This simulator takes inputs of satellite orbital elements, transmit signal properties, weather conditions, and receiver properties. As outputs it gives the estimated TDOA and its covariance, as well as the geometric solution and its covariance. This simulator has been used for further analysis, comparison, and optimization.

4.0 RESULTS AND DISCUSSION

The object of the research is to develop a passive and uncooperative satellite-based radio frequency localization platform that can be used to find the position of a transmitter that is located either on the earth or in orbit. To this end, time difference of arrival, frequency difference of arrival, and direction of arrival methods will be used. The research will include a thorough error analysis, and an investigation of the use of employing admissible regions to solve the space-to-space localization problem.

Figure 6 is a block diagram of this research. First, an ROI can be made based on access to the signal of the transmitter; the ROI could be conceivably used to optimize the deployment of the

RF localization satellite cluster—orbit optimization is not a part of this proposal. Next is the channel estimation portion, where the uncooperative signal and ephemeris data from the orbital model are combined with error modeling information. Then is the parameter estimation, where accumulation time is calculated and used to obtain the TDOA and FDOA measurements, as well as their respective covariances. The TDOA and FDOA measurements and covariances are used in the RF localization block, where the TDOA and FDOA equations are solved for position and covariance if the transmitter is terrestrial; and for position, velocity, and covariances if the transmitter is space-based. Estimation techniques can be used to further refine the solution if multiple point solutions are obtained. RF CAR can be used when there is not enough information to solve for the orbit in the space-to-space scenario; bounding the solution to a range of possible orbits, and potentially converging toward a single solution.

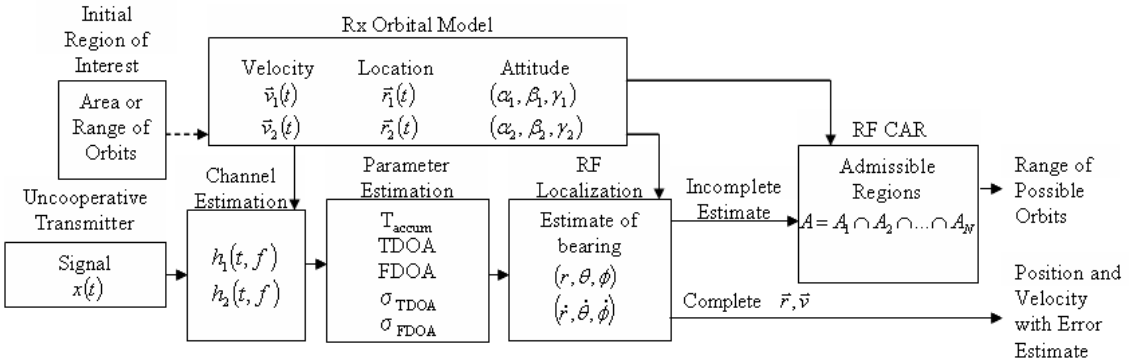

Figure 6. Block Diagram Describing the Proposed Method for Localizing a Space-Based Target from a Constellation of Spacecraft

In the space-to-space scenario, the transmitter orbital model is used to generate an ROI (for ground-to-space localization, other information is used to define the ROI), which again could be used for optimization of the RF localization satellite cluster. The transmitted signal at baseband is combined with information from the transmitter orbital model (space-to-space localization only) in the channel model with noise and interference added. The signal is then processed in the channel estimation block along with information from the receiver cluster orbital model. Information from the receiver orbital model is also used in the RF localization block. If not enough information is available for a solution, RF CAR is used to obtain a range of solutions using information from the receiver orbital model and the incomplete RF localization data. This process is shown in the block diagram in Figure 7.

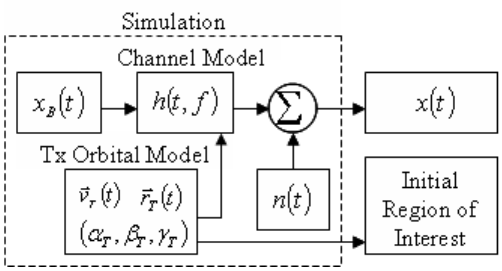

Figure 7. Block Diagram of the Simulation Process of this Project

4.1 Initial Region of Interest

The initial ROI is a very coarse estimate of where the transmitter is located. This region of interest can be used to know how and where to deploy the RF localization satellites, and possibly to determine if they are even necessary. In the future this initial region of interest could be incorporated into an optimization scheme of the overall problem. ROIs for four different transmission scenarios have already been developed.

4.2 Minimum Accumulation Time for Time Difference of Arrival and Frequency Difference of Arrival

It is necessary to know the minimum record time needed to obtain usable TDOA and FDOA measurements. This analysis has already been completed for TDOA; some more work could still be done for FDOA measurements.

Nearly all of the RF localization research that has been done thus far has concentrated on using the TDOA method. Much of this work also applies to the FDOA method, though there are some differences; some preliminary work has been done, but this should be explored further. The incorporation of FDOA measurements will also be important for space-to-space RF localization, as the FDOA measurements contain velocity information in addition to position information. This will consist of deriving and coding in Matlab an FDOA method of RF localization that could be used by alone or in conjunction with the existing TDOA RF localization method; and an expression for an FDOA measurement covariance will also be found or derived.

4.3 Comprehensive Error Analysis

A comprehensive error analysis is important to know how usable the measurements will be, how this will affect solution accuracy, and whether or not a given scenario is even feasible. The error analysis has been completed for TDOA measurements; more work is still needed for FDOA measurements.

While some preliminary work has been done on error in TDOA measurements, more could be done, and it is also desired to analyze error in FDOA measurements. Particularly, the inclusion of environmental effects into the end-to-end simulation is not yet complete, and more work could be done on more accurately modeling receiver and positioning error. Research could also be done on how the error in TDOA and FDOA measurements affect the overall positioning solution. This will consist of coding into Matlab more error sources for the TDOA error analysis, and exploring how the fundamental error sources affect FDOA measurements and coding this into MATLAB. An analysis of error in the overall position or position and velocity solution will also be done.

4.4 Space-to-Space Radio Frequency Localization

Space-to-space RF localization is a relatively unexplored area in the literature. This could be accomplished relatively quickly, given the work that has already been done on this problem. It is a more complicated problem than space-to-ground localization, because it becomes an orbit determination problem. To solve this problem a combination of TDOA and FDOA measurements will be used. It is possible to find the orbit of the transmitter using only TDOA or FDOA, but it will be faster and more accurate to use both.

Space-to-space RF localization is largely an unexplored area in the literature, but it has a lot of potential. It has many similarities with geolocation, but whereas geolocation is only concerned with finding a position—and possibly a velocity, though this is not being addressed here—space-to-space localization becomes an orbit determination problem. Both position and velocity information are required to find the position of the space-based transmitter. This will consist of deriving and coding into Matlab a method of RF localization to determine the position and velocity vectors of a space-based transmitter using information obtained from TDOA and/or FDOA measurements as well as existing orbit determination techniques.

4.5 Constrained Admissible Regions for Space-to-Space Radio Frequency Localization

In cases where the number of satellites or measurements is not available for conventional orbit determination in the space-to-space scenario, constrained admissible regions could be used. Admissible regions have been used for the past decade for orbit determination problems with optical measurements, when not enough information is available to employ conventional techniques. There has been some minimal work done on the application of admissible regions to RF measurements, but this area is very underexploited. This work will consist of deriving and coding in MATLAB a new method of constrained admissible regions for TDOA and FDOA measurements.

Constrained admissible regions are a relatively new area of research, and there has been very little literature published on applying the concept to RF localization. CAR could allow space-to-space localization using as few as two satellites. The concept of CAR will be applied to TDOA, FDOA, and DOA measurements. The admissible regions will be hyper-dimensional surfaces in geometric space and in velocity space. Each region will be comprised of a combination of TDOA and FDOA measurements, with coarse DOA measurements acting primarily as constraints. The specific composition of TDOA, FDOA, and DOA measurements will be dictated by the scenario, the number of satellites, and which satellites have access to the transmitter at the time the measurements are made. By forward propagating multiple admissible regions for various measurement times, an orbit solution could be converged on.

In the context of RF measurements, an admissible region can be obtained from a single TDOA, FDOA, or DOA measurement; however, if more than one of these measurements correspond to the same instant in time, these multiple measurements can be used to define a smaller admissible region. Four TDOA measurements at the same instant in time will yield an admissible region that is a point in space and all of velocity space (though, constrained by the energy of a closed orbit); three TDOA measurements at the same instant will yield an admissible region of two points in space and all of velocity space (again, constrained by the energy of a closed orbit); two TDOA measurements at the same instant will yield an admissible region that is like an ellipse in space, and all of velocity space; and a single TDOA measurement will yield an admissible region that will be a hyperboloid in space, and all of velocity space.

A smaller admissible region can be obtained intersecting admissible regions from multiple instants in time. In the simplest case where there are two four-TDOA admissible regions at two different instants in time, it is a simple matter of solving the two-body problem for two points in space and time. For two three-TDOA admissible regions at two different instants in time, the problem is not much more complex. If only one combination of points in space and time satisfies the two-body problem, the orbit could be determined with two admissible regions; if not, one more admissible region will likely be enough to disambiguate solutions. Two double-TDOA or two single-TDOA admissible regions from two different instants in time could be intersected by propagating sample orbits from the earlier admissible region forward to the time of the later admissible region, where the new smaller admissible region will consist only of orbits that can exist in both the later admissible region and the earlier admissible region that was propagated forward. Repeating this process multiple times with double and single TDOA admissible regions will never result in a single solution, however, it may well converge toward a single solution in most cases. Admissible regions involving FDOA measurements will also include velocity information, and different position information than is obtained from TDOA measurements. DOA measurements, which are much coarser than TDOA or FDOA measurements could still likely be used to further limit the spatial portion of the admissible region.

4.6 Comprehensive Space-Based Uncooperative Radio Frequency Localization End-to-End Simulation Capability

A goal of this research is to provide end-to-end simulation capabilities for ground-to-space and space-to-space RF localization using the techniques developed here.

5.0 CONCLUSIONS

The object of this research was to develop a passive and uncooperative satellite-based radio frequency localization platform that can be used to find the position of a transmitter that is located either on the earth or in orbit. To this end, time difference of arrival, frequency difference of arrival, and direction of arrival methods were used. The research included a thorough error analysis, and an investigation of the use of employing constrained admissible regions to solve the space-to-space localization problem.

The project resulted in an end-to-end system and simulation capabilities for both geolocation and space-to-space localization using a small cluster of cubesats. An initial region of interest is defined using what information about the transmitter location is available. Formulas have been found or derived for covariances and minimum signal accumulation times. This system includes through error modeling, with some novel error sources included in the simulation model. The application of admissible regions to radio frequency measurements for orbit determination shows promise, but still requires more development.

In terms of future work, more research could be done on employing constrained admissible regions for radio frequency measurement to solve the space-to-space localization problem, and the accuracy of using such a method. Optimization of the localization satellite's orbits to efficiently and effectively search the initial region of interest should also be done.

REFERENCES

[1] Huelsmeyer, C., "Wireless transmitting and receiving mechanism for electric waves," U.S. Patent 810,150, issued 16 January 1906.

[2] Adamy, D., **EW 101: A First Course in Electronic Warfare**, 1st ed., Artech House Radar Library, Artech House Publishers, Boston, MA, 2001, pp. 173-174.

[3] Didlake, R., Odinets, O., "Sputnik and Amateur Radio," URL: http://www.arrl.org:80/news/features/2007/09/28/03/?nc=1. Accessed 30 June 2017.

[4] Chung, T., and Carter, C.R., "Basic Concepts in the Processing of SARSAT Signals," *IEEE Transactions on Aerospace and Electronic Systems*, vol **23**, no. 2, Mar 1987, pp. 175-178.

[5] Hofmann-Wellenhof, B., Lichtenegger, H., and Wasle, E., **GNSS – Global Navigation Satellite Systems**, Springer Wien, New York, NY, 2008.

[6] Ho, K. C., and Chan, Y. T., "Solution and performance analysis of geolocation by TDOA," *IEEE Transactions on Aerospace and Electronic Systems*, vol **29**, no. 4, Oct 1993, pp. 1311-1322.

[7] Shuster, S., Sinclair, A. J., and Lovell, T. A., "Initial relative-orbit determination using heterogeneous TDOA," *2017 IEEE Aerospace Conference*, Big Sky, MT, 2017, pp. 1-7.

[8] Sinclair, A. J., Lovell, T. A., and Darling, J., "RF localization solution using heterogeneous TDOA," *2015 IEEE Aerospace Conference*, Big Sky, MT, 2015, pp. 1-7.

[9] Guo, F., Fan, Y., Zhou, Y., Xhou, C., and Li, Q., **Space Electronic Reconnaissance: Localization Theories and Methods**, 1st ed., John Wiley & Sons, Singapore, 2014.

[10] Swartwout, M., "Assessing the debris risk from the avalanche of CubeSats," *2016 IEEE Aerospace Conference*, Big Sky, MT, 2016, pp. 1-9.

[11] Milligan, T. A., **Modern Antenna Design**, 2nd ed., IEEE Press, Wiley-Interscience, John Wiley & Sons, Hoboken, NJ, 2005.

[12] Escobal, P. R., Ong, K. M., and Roos, O. V., "Range difference multilateration for obtaining precision geodetic and trajectory measurements," *Acta Astronautica*, vol **2**, 1975, pp. 481-495.

[13] Chan, Y. T., and Ho, K. C., "A simple and efficient estimator for hyperbolic location," *IEEE Transactions on Signal Processing*, vol **42**, no. 8, Aug 1994, pp. 1905-1915.

[14] Ho, K. C., and Chan, Y. T., "Geolocation of a known altitude object from TDOA and FDOA measurements," *IEEE Transactions on Aerospace and Electronic Systems*, vol **33**, no. 3, July 1997, pp. 770-783.

[15] Musicki, D., and Koch, W., “Geolocation using TDOA and FDOA measurements,” *2008 11th International Conference on Information Fusion*, Cologne, Germany, 2008, pp. 1-8.

[16] Okello, N., and Musicki, D., “Emitter Geolocation with Two UAVs,” *2007 Information, Decision and Control (IDC ’07)*, Adelaide, Australia, Feb 2007, pp. 254-259.

[17] Fletcher, F., Ristic, B., and Musicki, D., “Recursive estimation of emitter location using TDOA measurements from two UAVs,” *IEEE 10th International Conference on Information Fusion*, Québec, Canada, 2007, pp. 1-8.

[18] Dumas, S., Lovell, T. A., Sinclair, A. J., and Durgin, G. D., "Analysis of Error in Time Difference of Arrival Measurements Introduced by the Motion of Satellite-Based Receivers," *2017 IEEE Wireless in Space and Extreme Environments Conference*, Montreal, Québec, Canada, 2017.

[19] Levis, C. A., Johnson, J. T., Teixeira, F. L., **Radiowave Propagation: Physics and Applications**, 1st ed., John Wiley & Sons, Hoboken, NJ, 2010.

[20] Saakian, A., **Radio Wave Propagation Fundamentals**, 1st ed., Artech House, Boston, MA, 2011.

[21] Ippolito, L. J., “Propagation Effects Handbook for Satellite Systems Design,” NASA Publication 1082(04), 1989.

[22] Hahn, W. R., “Optimum estimation of a delay vector caused by a random field propagating across an array of noisy sensors,” Ph.D. dissertation, Dep. Elec. Eng., Univ. Maryland, College Park, Md., 1972. Reprinted by the Naval Ordnance Lab., Silver Spring, MD., as NOLTR 72-120, June 16, 1972.

[23] Hahn, W., and Tretter, S., "Optimum processing for delay-vector estimation in passive signal arrays," *IEEE Transactions on Information Theory*, vol **19**, no. 5, Sep 1973, pp. 608-614.

[24] Milani, A., Gronchi, G. F., Vitturi, M. d., and Knezevic, Z., “Orbit Determination with Very Short Arcs: I. Admissible Regions,” *Celestial Mechanics and Dynamical Astronomy*, vol **90**, no. 1-2, 2004, pp. 57–85.

[25] Milani, A., Gronchi, G. F., Knezevic, Z., Sansaturio, M. E., and Arratia, O., “Orbit determination with very short arcs: II. Identifications,” *Icarus*, vol **179**, no. 2, 2005, pp. 350-374.

[26] Fujimoto, K., Scheeres, D. J., Herzog, J., and Schildknecht, T., “Association of Optical Tracklets from a Geosynchronous Belt Survey via the Direct Bayesian Admissible Region Approach,” *Advances in Space Research*, vol **53**, no. 2, 2014, pp. 295-208.

[27] Maruskin, J. M., Scheeres, D. J., and Alfriend, K. T., “Correlation of Optical Observations of Objects in Earth Orbit,” *Journal of Guidance, Control, and Dynamics*, vol **32**, no. 1, 2009, pp. 194-209.

[28] Fujimoto, K., Maruskin, J., and Scheeres, D., “Circular and zero-inclination solutions for optical observations of Earth-orbiting objects,” *Celestial Mechanics and Dynamical Astronomy*, vol **106**, no. 2, 2010, pp. 157-182.

[29] Siminski, J., Montenbruck, O., Fiedler, H., and Schildknecht, T., “Short-Arc Tracklet Association for Geostationary Objects,” *Advances in Space Research*, vol **53**, no. 8, 2014, pp. 1184–1194.

[30] DeMars, K., Jah, M., and Schumacher, P., “Initial Orbit Determination using Short-Arc Angle and Angle Rate Data,” *IEEE Transactions on Aerospace and Electronic Systems*, vol **48**, no. 3, 2012, pp. 2628-2637.

[31] Hussein, I., Schumacher, P. W., Wilkins, M. P., Roscoe, C. W. T., "Probabilistic Admissible Region for Short-Arc Angles-only Observations," *2014 AMOS Conference*, Maui, Hawaii, 2014.

[32] DeMars, K. J., and Jah, M. K., “Probabilistic Initial Orbit Determination Using Gaussian Mixture Models,” *Journal of Guidance, Control, and Dynamics*, vol **36**, Sep–Oct 2013, pp. 1324-1335.

[33] Weisman, R. M., and Jah, M. K., “Uncertainty Quantification for Angles-Only Initial Orbit Determination,” *AAS/AIAA Spaceflight Mechanics Meeting*, Maui, Hawaii, Jan. 2014.

[34] Tommei, G., Milani, A., and Rossi, A., “Orbit Determination of Space Debris: Admissibile Regions,” *Celestial Mechanics and Dynamical Astronomy*, vol **97**, 2007, pp. 289-304.

[35] Fujimoto, K., and K. T. Alfriend, "Optical Short-Arc Association Hypothesis Gating via Angle-Rate Information," *Journal of Guidance, Control, and Dynamics*, vol **38**, no. 9, Sep. 2015.

[36] Farnocchia, D., Tommei, G., Milani, A., and Rossi, A., “Innovative methods of correlation and orbit determination for space debris,” *Celestial Mechanics and Dynamical Astronomy*, vol **107**, no. 1-2, 2010, pp. 169-185.

[37] Worthy, J. L., Holzinger, M. J., “Uncued Satellite Initial Orbit Determination Using Signals of Opportunity,” *AAS/AIAA Astrodynamics Specialist Conference*, Vail, CO, Aug. 2015.

[38] Klobuchar, J. A., "Ionospheric Time-Delay Algorithm for Single-Frequency GPS Users," *IEEE Transactions on Aerospace and Electronic Systems*, vol **3**, May 1987, pp. 325-331.

APPENDIX: SIMULATED DATA FROM ANALYSIS OF TDOA ERROR FROM SATELLITE MOTION

Tabulated in this appendix is the simulated data from the analysis of time difference of arrival error introduced from satellite motion.

Table A-1. Simulated Data

Simulation	*Simulation Parameters (Inputs)*					*Metric Parameters (Outputs)*				
	Transmitter: Longitude, Latitude, Signal	***Receiver 1 Orbital Elements at Epoch Time t_0***	***Receiver 2 Orbital Elements at Epoch Time t_0***	***Start and Stop Times of Record Interval and Accumulation Time***	***Sampling Frequency***	***TDOA at the Start of the Record Interval***	***TDOA at the End of the Record Interval***	***TDOA at the Center of the Record Interval***	***Correlated TDOA***	***TDOA Error***
Nominal Scenario	45º, 20º, 100 kHz Tone	a1 = 7010 km e1 = 0.03 i1 = 55° ω1 = 0° Ω1 = 0° f1 = 0°	a2 = 7010 km e2 = 0.03 i2 = 55° ω2 = 0° Ω2 = 0° f2 = 2°	T_{start} = 5840 s T_{stop} = 5841 s T_{accum} = 1 s	10 MHz	640.37 606 µs	639.80 851 µs	640.09 228 µs	640.07897 µs	13.32 ns
15 MHz Sampling Frequency	45º, 20º, 100 kHz Tone	a1 = 7010 km e1 = 0.03 i1 = 55° ω1 = 0° Ω1 = 0° f1 = 0°	a2 = 7010 km e2 = 0.03 i2 = 55° ω2 = 0° Ω2 = 0° f2 = 2°	T_{start} = 5840 s T_{stop} = 5841 s T_{accum} = 1 s	15 MHz	640.37 606 µs	639.80 851 µs	640.09 228 µs	640.07896 µs	13.33 ns
7 MHz Sampling Frequency	45º, 20º, 100 kHz Tone	a1 = 7010 km e1 = 0.03 i1 = 55° ω1 = 0° Ω1 = 0° f1 = 0°	a2 = 7010 km e2 = 0.03 i2 = 55° ω2 = 0° Ω2 = 0° f2 = 2°	T_{start} = 5840 s T_{stop} = 5841 s T_{accum} = 1 s	7 MHz	640.37 606 µs	639.80 851 µs	640.09 228 µs	640.07897 µs	13.32 ns
5 MHz Sampling Frequency	45º, 20º, 100 kHz Tone	a1 = 7010 km e1 = 0.03 i1 = 55° ω1 = 0° Ω1 = 0° f1 = 0°	a2 = 7010 km e2 = 0.03 i2 = 55° ω2 = 0° Ω2 = 0° f2 = 2°	T_{start} = 5840 s T_{stop} = 5841 s T_{accum} = 1 s	5 MHz	640.37 606 µs	639.80 851 µs	640.09 228 µs	640.07892 µs	13.36 ns
3 MHz Sampling Frequency	45º, 20º, 100 kHz Tone	a1 = 7010 km e1 = 0.03 i1 = 55° ω1 = 0° Ω1 = 0° f1 = 0°	a2 = 7010 km e2 = 0.03 i2 = 55° ω2 = 0° Ω2 = 0° f2 = 2°	T_{start} = 5840 s T_{stop} = 5841 s T_{accum} = 1 s	3 MHz	640.37 606 µs	639.80 851 µs	640.09 228 µs	640.07874 µs	13.55 ns
1.5 MHz Sampling Frequency	45º, 20º, 100 kHz Tone	a1 = 7010 km e1 = 0.03 i1 = 55° ω1 = 0° Ω1 = 0° f1 = 0°	a2 = 7010 km e2 = 0.03 i2 = 55° ω2 = 0° Ω2 = 0° f2 = 2°	T_{start} = 5840 s T_{stop} = 5841 s T_{accum} = 1 s	1.5 MHz	640.37 606 µs	639.80 851 µs	640.09 228 µs	640.07787 µs	14.42 ns
1.1 MHz Sampling Frequency	45º, 20º, 100 kHz Tone	a1 = 7010 km e1 = 0.03 i1 = 55° ω1 = 0° Ω1 = 0° f1 = 0°	a2 = 7010 km e2 = 0.03 i2 = 55° ω2 = 0° Ω2 = 0° f2 = 2°	T_{start} = 5840 s T_{stop} = 5841 s T_{accum} = 1 s	1.1 MHz	640.37 606 µs	639.80 851 µs	640.09 228 µs	640.07686 µs	15.42 ns
1 MHz Sampling Frequency	45º, 20º, 100 kHz Tone	a1 = 7010 km e1 = 0.03 i1 = 55° ω1 = 0° Ω1 = 0° f1 = 0°	a2 = 7010 km e2 = 0.03 i2 = 55° ω2 = 0° Ω2 = 0° f2 = 2°	T_{start} = 5840 s T_{stop} = 5841 s T_{accum} = 1 s	1 MHz	640.37 606 µs	639.80 851 µs	640.09 228 µs	640.07641 µs	15.88 ns

Simulation	*Simulation Parameters (Inputs)*					*Metric Parameters (Outputs)*				
	Transmitter: Longitude, Latitude, Signal	*Receiver 1 Orbital Elements at Epoch Time t_0*	*Receiver 2 Orbital Elements at Epoch Time t_0*	*Start and Stop Times of Record Interval and Accumulation Time*	*Sampling Frequency*	*TDOA at the Start of the Record Interval*	*TDOA at the End of the Record Interval*	*TDOA at the Center of the Record Interval*	*Correlated TDOA*	*TDOA Error*
0.9 MHz Sampling Frequency	45°, 20°, 100 kHz Tone	a1 = 7010 km e1 = 0.03 i1 = 55° ω1 = 0° Ω1 = 0° f1 = 0°	a2 = 7010 km e2 = 0.03 i2 = 55° ω2 = 0° Ω2 = 0° f2 = 2°	T_{start} = 5840 s T_{stop} = 5841 s T_{accum} = 1 s	0.9 MHz	640.37606 µs	639.80851 µs	640.09228 µs	640.07578 µs	16.50 ns
0.5 MHz Sampling Frequency	45°, 20°, 100 kHz Tone	a1 = 7010 km e1 = 0.03 i1 = 55° ω1 = 0° Ω1 = 0° f1 = 0°	a2 = 7010 km e2 = 0.03 i2 = 55° ω2 = 0° Ω2 = 0° f2 = 2°	T_{start} = 5840 s T_{stop} = 5841 s T_{accum} = 1 s	0.5 MHz	640.37606 µs	639.80851 µs	640.09228 µs	640.06834 µs	23.94 ns
0.2 MHz Sampling Frequency	45°, 20°, 100 kHz Tone	a1 = 7010 km e1 = 0.03 i1 = 55° ω1 = 0° Ω1 = 0° f1 = 0°	a2 = 7010 km e2 = 0.03 i2 = 55° ω2 = 0° Ω2 = 0° f2 = 2°	T_{start} = 5840 s T_{stop} = 5841 s T_{accum} = 1 s	0.2 MHz	640.37606 µs	639.80851 µs	640.09228 µs	640.00000 µs	92.29 ns
0.15 MHz Sampling Frequency	45°, 20°, 100 kHz Tone	a1 = 7010 km e1 = 0.03 i1 = 55° ω1 = 0° Ω1 = 0° f1 = 0°	a2 = 7010 km e2 = 0.03 i2 = 55° ω2 = 0° Ω2 = 0° f2 = 2°	T_{start} = 5840 s T_{stop} = 5841 s T_{accum} = 1 s	0.15 MHz	640.37606 µs	639.80851 µs	640.09228 µs	639.90444 µs	187.85 ns
0.1 MHz Sampling Frequency	45°, 20°, 100 kHz Tone	a1 = 7010 km e1 = 0.03 i1 = 55° ω1 = 0° Ω1 = 0° f1 = 0°	a2 = 7010 km e2 = 0.03 i2 = 55° ω2 = 0° Ω2 = 0° f2 = 2°	T_{start} = 5840 s T_{stop} = 5841 s T_{accum} = 1 s	0.1 MHz	640.37606 µs	639.80851 µs	640.09228 µs	3.60211415 ms	2.962021875 ms
1 kHz Transmit Frequency	45°, 20°, 1 kHz Tone	a1 = 7010 km e1 = 0.03 i1 = 55° ω1 = 0° Ω1 = 0° f1 = 0°	a2 = 7010 km e2 = 0.03 i2 = 55° ω2 = 0° Ω2 = 0° f2 = 2°	T_{start} = 5840 s T_{stop} = 5841 s T_{accum} = 1 s	10 MHz	640.37606 µs	639.80851 µs	640.09228 µs	640.03518 µs	57.10 ns
10 kHz Transmit Frequency	45°, 20°, 10 kHz Tone	a1 = 7010 km e1 = 0.03 i1 = 55° ω1 = 0° Ω1 = 0° f1 = 0°	a2 = 7010 km e2 = 0.03 i2 = 55° ω2 = 0° Ω2 = 0° f2 = 2°	T_{start} = 5840 s T_{stop} = 5841 s T_{accum} = 1 s	10 MHz	640.37606 µs	639.80851 µs	640.09228 µs	640.07874 µs	13.55 ns
1 MHz Transmit Frequency	45°, 20°, 1 MHz Tone	a1 = 7010 km e1 = 0.03 i1 = 55° ω1 = 0° Ω1 = 0° f1 = 0°	a2 = 7010 km e2 = 0.03 i2 = 55° ω2 = 0° Ω2 = 0° f2 = 2°	T_{start} = 5840 s T_{stop} = 5841 s T_{accum} = 1 s	10 MHz	640.37606 µs	639.80851 µs	640.09228 µs	640.07954 µs	12.75 ns
0.5 s Accumulation Time	45°, 20°, 100 kHz Tone	a1 = 7010 km e1 = 0.03 i1 = 55° ω1 = 0° Ω1 = 0° f1 = 0°	a2 = 7010 km e2 = 0.03 i2 = 55° ω2 = 0° Ω2 = 0° f2 = 2°	T_{start} = 5840 s T_{stop} = 5840.5 s T_{accum} = 0.5 s	10 MHz	6.4037606 µs	6.4009296 µs	6.4023451 µs	6.4022784 µs	6.67 ns
0.07 s Accumulation Time	45°, 20°, 100 kHz Tone	a1 = 7010 km e1 = 0.03 i1 = 55° ω1 = 0° Ω1 = 0° f1 = 0°	a2 = 7010 km e2 = 0.03 i2 = 55° ω2 = 0° Ω2 = 0° f2 = 2°	T_{start} = 5840 s T_{stop} = 5840.07 s T_{accum} = 0.07 s	10 MHz	6.4037606 µs	6.4033650 µs	6.4035628 µs	6.4035535 µs	0.93 ns

Simulation	*Simulation Parameters (Inputs)*					*Metric Parameters (Outputs)*				
	Transmitter: Longitude, Latitude, Signal	*Receiver 1 Orbital Elements at Epoch Time t_0*	*Receiver 2 Orbital Elements at Epoch Time t_0*	*Start and Stop Times of Record Interval and Accumulation Time*	*Sampling Frequency*	*TDOA at the Start of the Record Interval*	*TDOA at the End of the Record Interval*	*TDOA at the Center of the Record Interval*	*Correlated TDOA*	*TDOA Error*
Middle of Pass	45º, 20º, 100 kHz Tone	a1 = 7010 km e1 = 0.03 i1 = 55° ω1 = 0° Ω1 = 0° f1 = 0°	a2 = 7010 km e2 = 0.03 i2 = 55° ω2 = 0° Ω2 = 0° f2 = 2°	T_{start} = 6120 s T_{stop} = 6121 s T_{accum} = 1 s	10 MHz	-72.52386 μs	-77.49179 μs	-75.00782 μs	-75.00791 μs	0.09 ns
End of Pass	45º, 20º, 100 kHz Tone	a1 = 7010 km e1 = 0.03 i1 = 55° ω1 = 0° Ω1 = 0° f1 = 0°	a2 = 7010 km e2 = 0.03 i2 = 55° ω2 = 0° Ω2 = 0° f2 = 2°	T_{start} = 6390 s T_{stop} = 6391 s T_{accum} = 1 s	10 MHz	-674.0914 μs	-674.5210 μs	-674.3062 μs	-674.32029 μs	14.04 ns
Non-Tone Signal	45º, 20º, $\sum_{i=1}^{10}\sin\left(2\pi\frac{1}{-}\right.$	a1 = 7010 km e1 = 0.03 i1 = 55° ω1 = 0° Ω1 = 0° f1 = 0°	a2 = 7010 km e2 = 0.03 i2 = 55° ω2 = 0° Ω2 = 0° f2 = 2°	T_{start} = 5840 s T_{stop} = 5841 s T_{accum} = 1 s	10 MHz	640.37606 μs	639.80851 μs	640.09228 μs	640.07894 μs	13.34 ns
Thermal Noise Added	45º, 20º, 100 kHz Tone	a1 = 7010 km e1 = 0.03 i1 = 55° ω1 = 0° Ω1 = 0° f1 = 0°	a2 = 7010 km e2 = 0.03 i2 = 55° ω2 = 0° Ω2 = 0° f2 = 2°	T_{start} = 5840 s T_{stop} = 5841 s T_{accum} = 1 s	10 MHz	640.37606 μs	639.80851 μs	640.09228 μs	640.07245 μs	19.83 ns
Another Scenario	45º, 20º, 100 kHz Tone	a1 = 7010 km e1 = 0.03 i1 = 55° ω1 = 0° Ω1 = 0° f1 = 0°	a2 = 8010 km e2 = 0.3 i2 = 75° ω2 = 0° Ω2 = 0° f2 = 2°	T_{start} = 37330 s T_{stop} = 37331 s T_{accum} = 1 s	10 MHz	-9.35269075 ms	-9.34157860 ms	-9.34713468 ms	-9.34714762 ms	12.94 ns

LIST OF ACRONYMS, ABBREVIATIONS, AND SYMBOLS

AFRL	Air Force Research Laboratory
CRLB	Cramer-Rao Lower Bound
CST	Computer Simulation Technology
DOA	Direction of Arrival
FCC	Federal Communications Commission
FDOA	Frequency Difference of Arrival
FROA	Frequency Ratio on Arrival
GLONASS	Globalnaya Navigazionnaya Sputnikovaya Sistema
GNSS	Global Navigation Satellite System
GPS	Global Positioning System
HEML	High-Energy Electromagnetics Laboratory
LEO	Low Earth Orbit
NAVSAT	Navy Navigation Satellite System
RF	Radio Frequency
ROI	Region of Interest
SARSAT	Search And Rescue Satellite-Aided Tracking
SNR	Signal to Noise Ratio
TDOA	Time Difference of Arrival

DISTRIBUTION LIST

DTIC/OCP 8725 John J. Kingman Rd, Suite 0944 Ft Belvoir, VA 22060-6218	1 cy
AFRL/RVIL Kirtland AFB, NM 87117-5776	1 cy
Official Record Copy AFRL/RVSV/Thomas Lovell	1 cy